

RESEARCH ARTICLE

WILEY

Increases in aridity lead to drastic shifts in the assembly of dryland complex microbial networks

Manuel Delgado-Baquerizo^{1,2} | Guilhem Doulier^{3,4} | David J. Eldridge⁵ |
Daniel B. Stouffer⁴ | Fernando T. Maestre⁶ | Juntao Wang² |
Jeff R. Powell² | Thomas C. Jeffries² | Brajesh K. Singh^{2,7}

¹Cooperative Institute for Research in Environmental Sciences, University of Colorado, Boulder, CO

²Hawkesbury Institute for the Environment, Western Sydney University, Penrith, New South Wales, Australia

³Institut de Biologie de l'École Normale Supérieure, École Normale Supérieure, PSL Research University, Paris, 75005, France

⁴Centre for Integrative Ecology, School of Biological Sciences, University of Canterbury, Christchurch, New Zealand

⁵Centre for Ecosystem Science, School of Biological, Earth and Environmental Sciences, University of New South Wales, Sydney, New South Wales, Australia

⁶Departamento de Biología, Geología, Física y Química Inorgánica, Escuela Superior de Ciencias Experimentales y Tecnología, Universidad Rey Juan Carlos, Móstoles, Spain

⁷Global Centre for Land-Based Innovation, Western Sydney University, Penrith South DC, New South Wales, Australia

Correspondence

M. Delgado-Baquerizo, Cooperative Institute for Research in Environmental Sciences, University of Colorado, Boulder, CO 80309.
Email: m.delgadobaquerizo@gmail.com

Funding information

Alexander von Humboldt Foundation; Ministerio de Economía y Competitividad, Grant/Award Number: CGL2013-44661-R; European Research Council, Grant/Award Number: 647038; Hermon Slade Foundation; Marie Skłodowska-Curie Actions of the Horizon 2020 Framework Programme, Grant/Award Number: 702057; Rutherford Discovery Fellowship; Marsden Fast-Start Grant; Australian Research Council, Grant/Award Numbers: DP170104634, DP190103714

Abstract

We have little information on how and why soil microbial community assembly will respond to predicted increases in aridity by the end of this century. Here, we used correlation networks and structural equation modeling to assess the changes in the abundance of the ecological clusters including potential winner and loser microbial taxa associated with predicted increases in aridity. To do this, we conducted a field survey in an environmental gradient from eastern Australia and obtained information on bacterial and fungal community composition for 120 soil samples and multiple abiotic and biotic factors. Overall, our structural equation model explained 83% of the variance in the two mesic modules. Increases in aridity led to marked shifts in the abundance of the two major microbial modules found in our network, which accounted for >99% of all phylotypes. In particular, the relative abundance of one of these modules, the Mesic Module #1, which was positively related to multiple soil properties and plant productivity, declined strongly with aridity. Conversely, the relative abundance of a second dominant module (Xeric Module #2) was positively correlated with increases in aridity. Our study provides evidence that network analysis is a useful tool to identify microbial taxa that are either winners or losers under increasing aridity and therefore potentially under changing climates. Our work further suggests that climate change, and associated land degradation, could potentially lead to extensive microbial phylotypes exchange and local extinctions, as demonstrated by the reductions of up to 97% in the relative abundance of microbial taxa within Mesic Module #1.

KEYWORDS

bacteria, climate change, ecological networks, fungi, global change ecology, plant–soil interactions, soil functions

1 | INTRODUCTION

Climate change is leading to a drier and hotter world and resulting in major soil degradation processes (Huang, Yu, Guan, Wang, & Guo, 2016). Drylands already occupy over 45% of Earth's landmass, with their cover expected to further increase by up to 23% by the end of this century (Huang et al., 2016). In drylands, soil bacteria and fungi are the most diverse and abundant organisms and play critical roles in maintaining the rates and stability of multiple ecosystem functions, including litter decomposition, primary production, soil fertility, and gas exchange (Delgado-Baquerizo et al., 2017). However, the diversity and abundance of fungi and bacteria are also highly vulnerable to climate change (Maestre et al., 2015). Microbial communities exhibit complex connections involving a large number of interdependent and intradependent interactions, making it very difficult to predict how the entire microbial communities are likely to respond to global environmental change (Rillig et al., 2015; Shi et al., 2016). Some taxa can potentially benefit from increases in aridity (winners), whereas other taxa will be hindered as aridity increases (losers; *sensu* Eldridge, Delgado-Baquerizo, Travers, Val, & Oliver, 2018). Identifying potential winner and loser taxa in response to increases in aridity could have potential future implications for the management of microbial communities under global change scenarios. Network analysis has recently been proposed as a promising approach to describe this complexity and to obtain deeper insights into the organization of microbial associations in terrestrial ecosystems (Shi et al., 2016). The structure of ecological networks, which integrates biodiversity, community composition, and ecosystem functioning (Tylianakis et al., 2008), is also regarded as a key attribute of biotic communities. Thus, taking a whole-network approach has the potential to advance our knowledge of microbial community and ecosystem responses to global change drivers (e.g., climate change) at both local and global scales (Barberán, Bates, Casamayor, & Fierer, 2012; Neilson et al., 2017; Rillig et al., 2015).

Recent studies have demonstrated that soil microbial taxa strongly associate with each other and lead to the formation of well-defined modules (nodes of fungi or bacteria, also called as ecological clusters) of taxa, providing evidence for tightly synchronized responses among bacteria and fungi (Shi et al., 2016). Moreover, the previous studies have provided evidence that specific taxa of fungi and bacteria can share certain environmental preferences (Barberán et al., 2012; Rillig et al., 2015). Thus, they share similar predictors, such as location (distance from the equator), climate (e.g., aridity and temperature), and soil properties (e.g., pH and nutrients; Maestre et al., 2015; Ramirez et al., 2014; Tedersoo et al., 2014). This suggests that particular bacterial and fungal taxa may strongly co-occur in soils across environmental gradients. Unlike traditional analyses, more focus on the microbial diversity and community composition and the identification of highly connected modular structures representing important ecological units (Shi et al., 2016; Delgado-Baquerizo et al., 2018) provide a unique opportunity to integrate highly multidimensional data (i.e., such as those from microbial communities), allowing more robust statistical inferences on the major predictors of the entire microbial communities (Duran-Pinedo et al., 2011; Shi et al., 2016).

Microbial modules have recently been reported to represent highly dynamic ecological structures that respond to changing environmental conditions. For example, Nuccio et al. (2016) and Shi et al. (2016) showed that the modularity of microbial networks from plant rhizospheres responds to biological activity during a growing season. Much less is known, however, about how changes in climate, such as predicted increases in aridity (Huang et al., 2016), affect the network of associations among bacterial and fungal taxa within drylands (Neilson et al., 2017). Increasing aridity may alter the relative abundance of modules both directly (i.e., via reductions in water availability; Maestre et al., 2015) and indirectly (via changes in soil properties and plant attributes; Delgado-Baquerizo et al., 2016). For example, increases in soil pH associated with increasing aridity can influence the diversity and community composition of soil bacteria and fungi (Rousk et al., 2010; Maestre et al., 2015) and as such could affect soil microbial networks.

Here, we applied network analyses and statistical modeling to data from a regional survey (>1,000 km) spanning a wide range of aridity conditions and three within-plot vegetation types (Figure 1) to test the hypothesis that increases in aridity such as those forecasted under climate change will result in substantial shifts in the relative abundance of microbial modules, leading to a new network of microbial associations in soils in ecosystems from eastern Australia. More importantly, we aim to identify a list of winner and loser taxa in response to potential increases in aridity in eastern Australia (Huang et al., 2016).

2 | MATERIALS AND METHODS

2.1 | Study area

We conducted this study at 20 locations from eastern Australia (Figure 1a). Locations for this study were chosen to include a wide range of aridity levels including arid, semiarid, and dry-subhumid ecosystems. The total annual precipitation and mean temperature in this region ranged from 280 to 1,167 mm and from 12.8 to 17.5°C, respectively. The locations included in this study showed a wide variety of vegetation types (e.g., grasslands, shrublands, savannas, dry seasonal forests, and open woodlands dominated by trees). Perennial plant cover in these plots ranged from 18 to 98%.

2.2 | Soil sampling

Soils were sampled in the Australian summer (March 2014). Within each site, we selected a 30 m × 30 m plot, which represented the dominant vegetation within each location. Plant cover and richness were measured within each plot as explained in Maestre et al. (2015). We collected three composite soil samples (three 0- to 5-cm-depth soil cores) from beneath the vegetation (N-fixing shrubs, grasses, and trees) and in open areas between plant patches at each site. The same plant taxa were present across the complete gradient of aridity: *Eucalyptus* spp., *Acacia* spp., and the C3 native grass *Rhynchospora* spp. A total of 120 soil samples (20 sites × 6 within-plot composite samples)

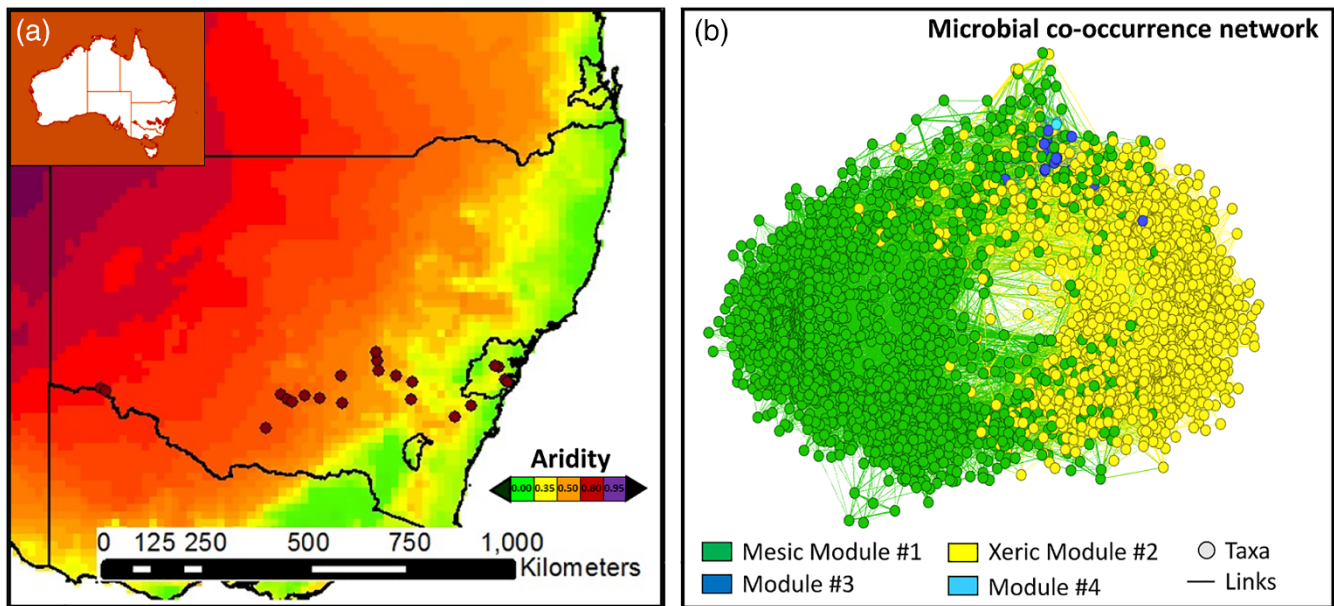


FIGURE 1 Location of the study sites studied (a) and correlation network including multiple nodes (taxa) from bacteria and fungi (b). Color patterns in panel (a) indicate aridity (1–AI) gradients. Different colors in panel (b) correspond with different modules

were collected in this study. Note that we used a stratified sampling design to maximize within-plot spatial variability, which is critical for building co-occurrence networks based on correlations. Our sampling design also allows the comparison of information collected across plots, which otherwise (i.e., random sampling design) might have differed in terms of spatial variability. Soil samples were sieved (2-mm mesh). Then, portion of soil was immediately frozen at -20°C for molecular analyses, whereas the rest of the soil was air-dried and stored for 1 month before physicochemical analyses.

2.3 | Soil properties

Soil total organic C content was determined using the method described in Maestre et al. (2015). Soil total N was measured with a CNH analyzer (Leco CHN628 Series, LECO Corporation, St Joseph, MI). Soil pH was measured in all the soil samples (1, 2.5 soil or water suspension). Total p was measured after digestion with sulphuric acid using a SKALAR San++ Analyzer (Skalar, Breda, the Netherlands). Soil total p was positively and significantly correlated with microbial biomass p ($\rho = .18$; $p = .049$), Olsen inorganic p ($\rho = .45$; $p < .001$), and plant leaf p content ($\rho = .23$; $p = .027$) and, therefore, is a good surrogate of p availability. Total p ranged from 17 to 600 mg P kg $^{-1}$ soil. Soil total organic C ranges from 0.7 to 12%. Soil pH ranged from 4.8 to 9.1%.

2.4 | Surrogates of ecosystem functioning

We measured (a) the activities of three soil enzymes using the method explained in Bell et al. (2013): α -glucosidase (starch degradation), N -acetyl- β -glucosaminidase (chitin degradation), and phosphatase (organic phosphorus mineralization); (b) the availability of dissolved organic carbon and inorganic N from K_2SO_4 extracts measured as

described in Delgado-Baquerizo et al. (2016); and (c) aboveground net primary productivity (ANPP) for the whole of 2014 and for March 2014, the month in which soil sampling was conducted using NDVI obtained from satellite data as described in Delgado-Baquerizo et al. (2018).

2.5 | Environmental variables

For each site, we calculated the aridity level (1–aridity index [AI], where AI is precipitation or potential evapotranspiration) using AI data from the database in Maestre et al. (2015). We used aridity rather than mean annual precipitation because aridity is a more appropriate variable that includes both mean annual precipitation and potential evapotranspiration. Furthermore, this variable provides an integrative measure of the long-term water availability at each site. Finally, we identified the soil type in each plot using available data from the International Soil Reference and Information Centre Soil Grids—global gridded soil information (https://soilgrids.org/#/?layer=geonode:taxnwr_b_250m), which provide global information on soil classification United States Department of Agriculture (USDA classification) at a 250-m resolution.

2.6 | Molecular analyses

Soil DNA was extracted from 0.25 g of soil samples (defrosted) using the Powersoil DNA Isolation Kit (Mo Bio Laboratories, Carlsbad, CA). We quantified the total abundance bacteria and fungi in all soil samples using 96-well plates on a CFX96 Touch Real-Time Polymerase chain reaction (PCR) Detection System (Foster City, CA; qPCR). We used the primer sets: Eub 338–Eub 518 and Internal transcribed spacer (ITS) 1–5.8S described in Maestre et al. (2015) for qPCR analyses. We then employed amplicon sequencing using the Illumina

MiSeq platform to characterize the community composition of bacteria and fungi in our samples. We used the 341F/805R (bacteria) and FITS7/ITS4 (fungi) primer sets (Maestre et al., 2015) for these analyses. Bioinformatic processing was performed using a combination of Quantitative Insights into Microbial Ecology (Caporaso et al., 2010), USEARCH (Edgar, 2010), and UCLUST (Edgar, 2010). Operational taxonomic units (phylotypes hereafter) were defined as clusters of 97% sequence similarity using UCLUST (Edgar, 2010). Taxonomy was assigned using against the Greengenes database version 13_850 for 16S rDNA operational taxonomic units (DeSantis et al., 2006). For fungal ITS sequences, taxonomy was assigned using the UNITE database V6.9.7 ($E < 10^{-5}$; Koljalg et al., 2013). We filtered the Operational taxonomic unit (OTU) abundance tables for both primer sets to remove singletons. We then rarefied to an even number of sequences per samples to ensure an equal sampling depth (11,789 and 16,222 for 16S rDNA and ITS, respectively).

2.7 | Network analyses

We first built a single correlation network between the phylotypes within the abundance table using the following protocol aiming to identify modules of strongly co-occurring microbial taxa. Prior to these analyses, we filtered out the rarest phylotypes by removing those with less than five reads in at least one sample across all samples. This resulted in a network with 25,084 phylotypes as nodes (10,570 bacterial and 14,514 fungal phylotypes, respectively). We then calculated all pairwise Spearman correlation coefficients among these microbial taxa and kept all positive correlations. This nonparametric method measures the strength and direction of association between two ranked variables. We focused exclusively on positive correlations because they provide useful information on the co-occurrence of particular microbial taxa that may respond in a similar manner to particular environmental conditions such as increases in aridity (Barberan et al., 2012). This approach ultimately allowed us to address our research question on the role aridity in regulating the relative abundance of the main microbial modules composed by bacterial and fungal taxa strongly co-occurring with each other. This led to a network with 62,388,880 links, which corresponds to just 19.8% of all possible links (falling within the expected range from the previous ecological networks; Stouffer & Bascompte, 2011). In all instances, we weighted these links by their corresponding correlation coefficient. We then used the Markov Cluster Algorithm software (van Dongen, 2000) to extract modules from the network. This algorithm is explicitly designed to efficiently handle large networks. Here, a single parameter controls the quality of the clustering output. Rather than using the default options, we adjusted the inflation parameter to maximize the modularity of the resulting partition, which is a quantitative measure of the quality of a given partitioning of nodes in a network (Newman & Girvan, 2004). We used an inflation parameter $l = 2.8$, which lead to a maximum modularity $M = 0.124951$ based on the assignment of phylotypes to four separate modules. We then calculated the relative abundance of these modules by summing the relative abundances (%) of all phylotypes within each module. Finally, we

computed the relative abundance of each module in each site as the average relative abundance in the site's samples weighted by the coverage of the corresponding microhabitats (vegetation and open areas). Using this approach, we focus on the relative abundance of modules rather than on individual taxa.

After obtaining this co-occurrence network and detecting the modules within this network, we proceeded to cross-validate our network using an independent approach. To do this, we first calculated all pairwise Sparse Correlations for Compositional (SparCC) correlations between bacterial and fungal nodes using the Fastspat algorithm (Friedman & Alm, 2017), with 100 bootstraps and 100 permutations to control false discovery rate. For these analyses, we used a more conservative approach than that described above and used a minimum correlation coefficient of 0.4 and $p < .05$. Finally, we used the algorithm introduced by Vincent, Larochelle, Bengio, and Manzagol (2008) to extract modules from the network. The relative abundance of these modules was calculated as the average of the standardized relative abundances (z-score) of all phylotypes within each module.

2.8 | Statistical analyses

We evaluated the effect of aridity on the relative abundance of different microbial clusters (or modules) using linear regressions. To account for the spatial influence of the data (latitude and longitude), we used spatial autoregressive analyses. We used structural equation modeling (SEM, Grace, 2006) to evaluate the direct and indirect effects of aridity and other important predictors of soil microbial communities like the distance from the equator, soil type, and properties (total C, P, and pH), within-plot vegetation type (trees, shrubs, and grasses), plant cover and richness, and microbial attributes (fungal and bacterial abundance and ratio), on the relative abundance of detected microbial modules. Thus, we used SEM to further clarify the effects of aridity on the relative abundance of each microbial module after taking into account statistically the various environmental factors simultaneously (see our a priori model in Figure S1). Changes in soil properties, plant attributes, and microbial abundance due to increasing aridity could potentially affect the role that the environment plays in microbial associations, and this will likely influence the assembly of microbial networks in terrestrial environments. Furthermore, increases in aridity have been shown to reduce soil microbial abundance (Maestre et al., 2015), to decouple nutrient cycles (Delgado-Baquerizo et al., 2013), and to raise abiotic stress in drylands (Vicente-Serrano et al., 2012). Thus, soil properties, plant community attributes, and microbial abundance need to be considered when evaluating the role of increasing aridity as a driver of microbial community assembly.

Before conducting SEMs, soil total organic C and total phosphorus were log-transformed to improve linearity. Microbial abundance was introduced in the model as the average of the abundance of bacteria and fungi (after \log_{10} -transformation and z-score standardization). We did so to allow the inclusion of the fungal:bacterial ratio in our model, which otherwise would be highly correlated with the abundance of total bacteria and fungi. Note that we included this ratio in our model to provide further evidence that changes in the contribution from

fungal and bacterial phylotypes to each module considered the abundance of these organisms. Soil organic C was highly related to soil total N (Spearman's $\rho = .820$; $p < .001$), and its inclusion represented soil organic matter in our models (Delgado-Baquerizo et al., 2013). Because of this, total N was not explicitly included in the model. In our SEM model, the different within-plot vegetation types (grasses, N-fixing shrubs, and trees) were categorical variables with two levels: 1 (particular microhabitat; e.g., trees) and 0 (remaining microhabitats + open areas). Doing so allowed for comparison in the effect of a specific within-plot vegetation type (e.g., trees) on each microbial module with the average of the remaining vegetation types and open areas. Note that for our baseline condition (i.e., procedural control), we selected the composite samples from open areas and, therefore, did not explicitly include it in our model (Grace, 2006). Using the same approach, we included in our model the most common soil types: Ustox (Oxisols of semiarid and subhumid climates) and Albolls (Mollisols of wet soils), which were found in 95% of our studied sites.

We then tested model goodness of fit using the chi-square (χ^2) test. A model has a good fit when $0 \leq \chi^2 \leq 2$ and $0.05 < p \leq 1.00$ and the root mean square error of approximation (RMSEA; the model has a good fit when $RMSEA \leq 0.05$ and $0.10 < p \leq 1.00$). We

then used the Bollen–Stine bootstrap test (the model has a good fit when $0.10 < \text{bootstrap } p \leq 1.00$) to confirm model fit and our results indicated that our a priori model had a good fit to our data.

Finally, we used Spearman correlations to identify particular microbial taxa within a given module that are highly characteristic of particular aridity conditions (i.e., increase or decrease with aridity). In particular, we correlated the relative abundance of all phylotypes within each major module and aridity. These analyses were conducted using the R statistical software (<http://cran.r-project.org/>). Spearman correlations were also used to explore the link between the relative abundance of a given module and surrogates of multiple ecosystem functions including soil enzyme activities, available nutrients, and ANPP.

3 | RESULTS

We found that communities of fungi and bacteria are grouped into four largely independent microbial modules across our environmental gradient, accounting for 41.7, 57.7, 0.50, and 0.09% of the microbial phylotypes, respectively (Figure 1b). Each module represented a discrete, tightly correlated microbial cluster, including phylotypes of both

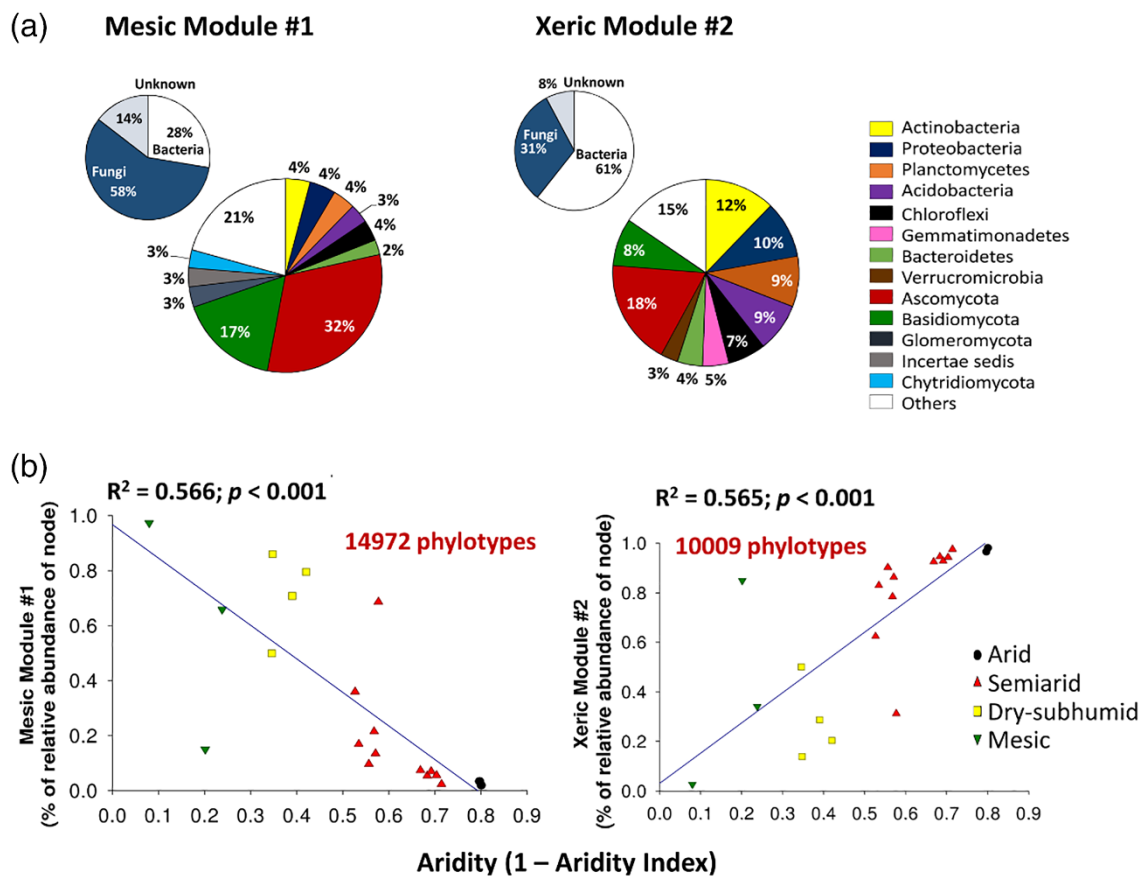


FIGURE 2 Community composition and association with increases in aridity for Mesic Module #1 and Xeric Module #2. Panel (a) shows the overall bacterial and fungal community composition for Mesic Module #1 and Xeric Module #2. Panel (b) shows the relationships between aridity and the relative abundance of microbial modules at the site level. Results of regressions are as follows: Mod#1. Ordinary least squares (OLS; continuous line), $R^2 = .566$, $p < .001$, AICc = 6.184; spatial autoregressive analyses (SAR), $R^2 = .451$, $p = .001$, AICc = 10.847; Mod#2. OLS (continuous line), $R^2 = .565$, $p < .001$, AICc = 6.251; SAR, $R^2 = .453$, $p = .001$, AICc = 10.819. Separate regressions at the sample level are shown in Figure S3

fungi and bacteria whose relative abundance was more strongly associated with each other than with phylotypes from other clusters (Figure 2). We retained in our network analyses the first three modules, which accounted for 99.9% of microbial phylotypes. Module #4 was not ubiquitous (i.e., it was present at only one site) and was therefore removed from further statistical modeling. The relative abundances of Modules #1 and #2 were highly negatively correlated ($\rho = -.999$; $p < .001$). Modules 1 ($\rho = .276$; $p = .002$) and 2 ($\rho = .283$; $p = .002$) were also related to Module #3. Modules #1 and #3 were dominated by fungal taxa, whereas Module #2 had a higher relative contribution from bacteria (Figures 2 and S1). Module #1 comprised 28% phylotypes of bacteria and 58% phylotypes of fungi, and Module #2 comprised 61% phylotypes of bacteria and 31% phylotypes of fungi (Figure 2a).

Aridity was strongly negatively and strongly positively related to the relative abundance of Module #1 (hereafter Mesic Module #1; defined as microbial taxa preferring more mesic environments) and #2 (hereafter Xeric Module #2; defined as microbial taxa preferring more arid environments), respectively, accounting for 99.4% of all taxa in all locations across our environmental gradient (i.e., standardized by microsite coverage; Figure 2a,b). Module #3 was not significantly related to aridity (Figures S2 and S3). Similar results were found at the sample level (Figure S3). These results were maintained when we controlled for the spatial influence of the data (Figure 2b). The relative abundances of Mesic Module #1 and Xeric Module #2 were strongly positively related to the relative abundances of the same modules but calculated as the standardized sum of the relative abundance of each OTU within each module (Spearman $\rho > .94$; $p < .001$). Moreover, similar results were found for the cross-validation network. The SparCC

Module #1 was significantly and positively related to Mesic Module #1 (Pearson's $r = .47$; $p < .001$), and SparCC Module #2 was significantly and positively related to Xeric Module #1 (Pearson's $r = .50$; $p < .001$). The SparCC analyses yielded an additional dominant module (SparCC Module #3), which was also significantly and positively correlated to Mesic Module #1 (Pearson's $r = .34$; $p < .001$). More importantly, SparCC Module #1 was negatively related to aridity (Pearson's $r = .27$; $p = .003$), whereas SparCC Module #2 was positively related to aridity (Pearson's $r = .50$; $p = .004$).

Overall, our structural equation model explained 83% of the variation in both Mesic Module #1 and Xeric Module #2. Aridity had a direct negative effect on the relative abundance of Mesic Module #1, while having a positive effect on the relative abundance of Xeric Module #2 (Figure 3a). Moreover, although the impacts of aridity on the relative abundance of the main modules were largely direct, we also found that increases in aridity affected the assembly of the microbial correlation network indirectly by shifting soil types from Albolls to Ustox, declining total plant cover and by increasing soil total P and pH (Figure 3a). We also found some direct and indirect effects of vegetation type on the relative abundance of microbial modules (Figure 3a). For example, the presence of trees had indirect negative and positive effects on Mesic Module #1 and Xeric Module #2, respectively, via soil pH and P. The relative abundance of Mesic Module #1 was positively correlated with multiple surrogates of ecosystem functioning, including nutrient availability, enzyme activities, and plant primary productivity (Table S1).

In general, we found that 2,806 and 4,676 microbial phylotypes within Mesic Module #1 and Xeric Module #2 were negatively and positively correlated with aridity, respectively ($p < .05$; Table S2). In

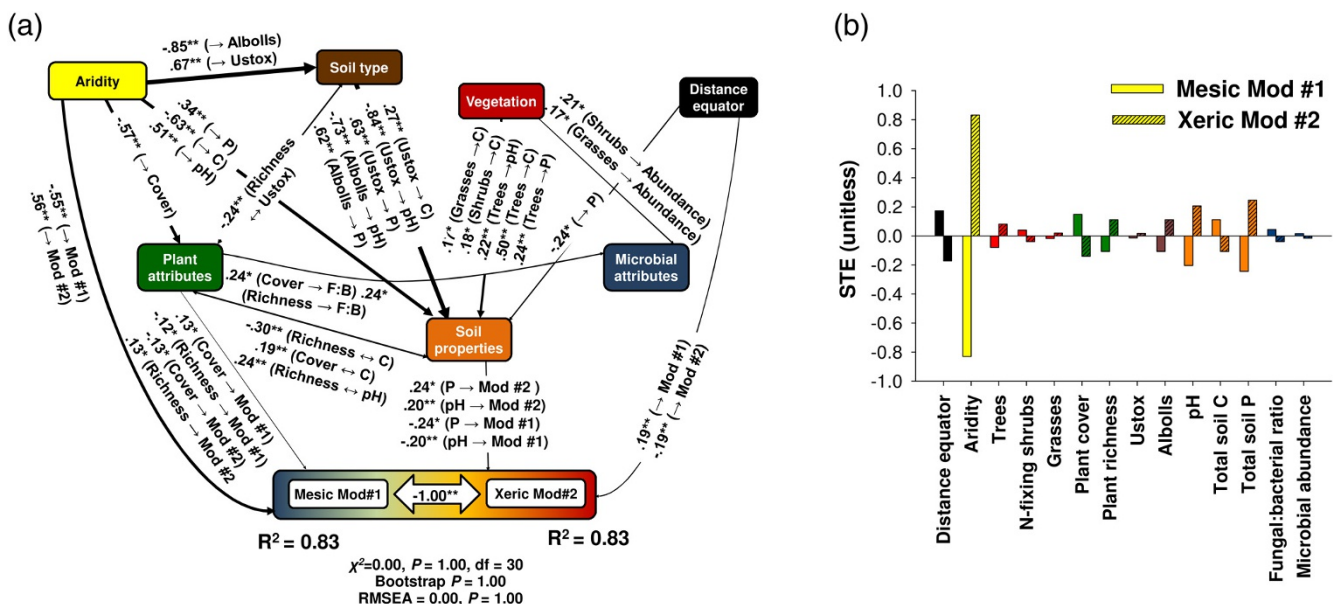
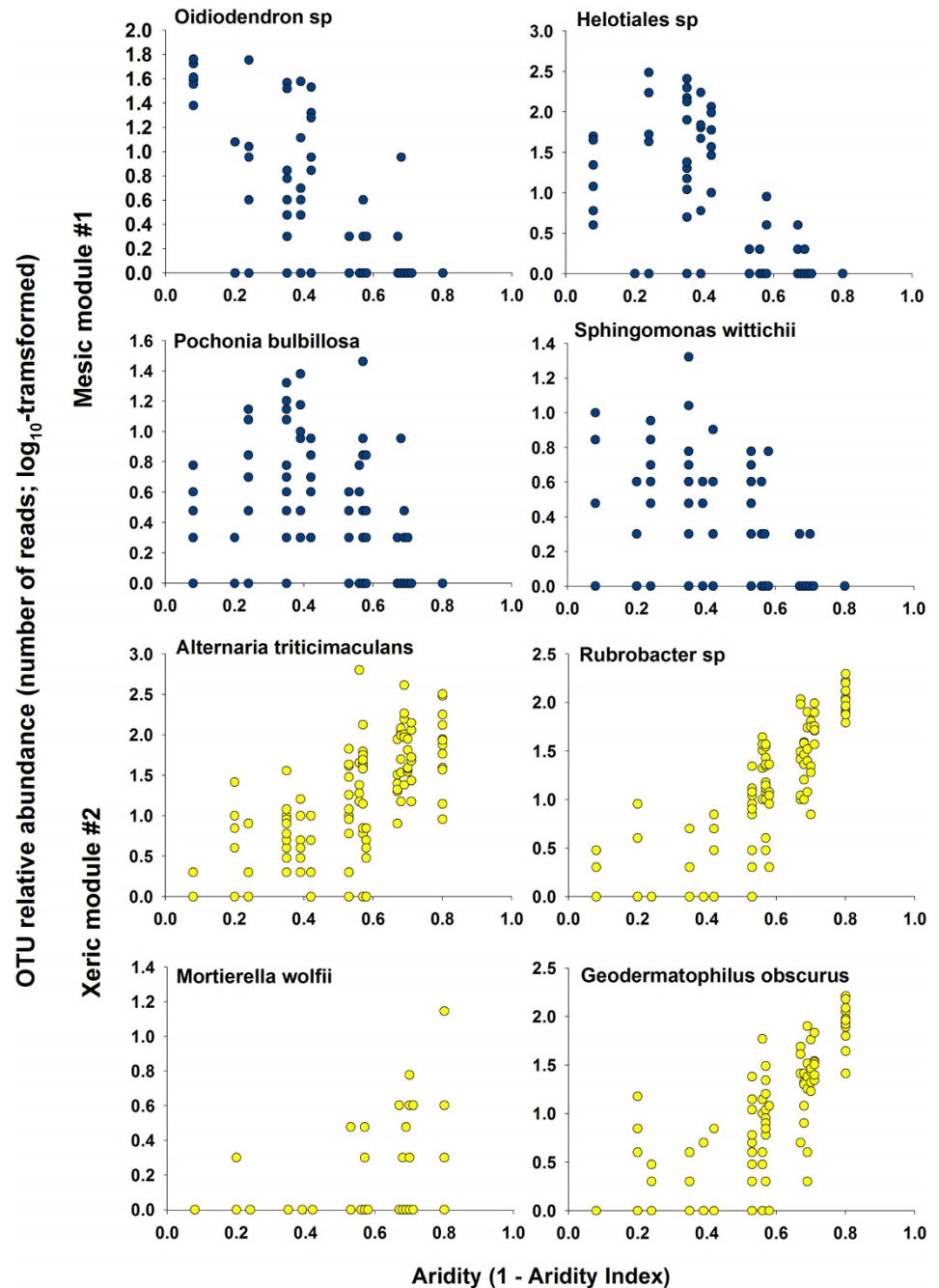


FIGURE 3 Structural equation model fitted to the relative abundance of microbial Modules #1 and #2 (a) and standardized total effects (direct plus indirect effects) derived from them (b). Numbers adjacent to arrows are path coefficients (p values) and are indicative of the effect size of the relationship. R^2 = the proportion of variance explained. P = soil total P; C = soil total organic C; F:B ratio = fungal:bacterial ratio. Vegetation = within-plot vegetation type (trees, shrubs, and grasses). Mods #1 and #2 = Mesic Module #1 and Xeric Module #2, respectively; p values are as follows: * $p < .05$; ** $p < .01$

FIGURE 4 Relationships between aridity and the relative abundance of selected phylotypes within Mesic Module #1 and Xeric Module #2. A more completed list of examples for phylotypes within Mesic Module #1 and Xeric Module #2 and their correlation (Spearman) to aridity is available in Table S2



particular, we found multiple microbial taxa from genus *Rubrobacter*, *Geodermatophilus*, and *Streptomyces* or class *Thermomicrobia* and phylotypes *Preussia minima*, *Alternaria triticimaculans*, *Pleosporales* sp., *Fusarium tricinctum* and *Phoma macrostoma*, *Tulostoma melanocyclum*, *Geastrum pectinatum*, *Laccaria* sp., and *Mortierella wolfii* to be strongly positively related to aridity (potential winners; Figure 4; Table S2). On the contrary, we found that microbial phylotypes including *Cladophialophora* sp., *Trichoderma spirale*, *Oidiodendron* sp., *Helotiales* sp., *Pochonia bulbillosa*, *Umbelopsis gibberispora* and *isabellina*, *Burkholderia tuberum*, *Sphingomonas wittichii*, *Mycobacterium celatum*, and *Actinomadura vinacea* were strongly negatively correlated with aridity (potential losers; Figure 4; Table S2). The complete list of taxa predicting aridity changes within each module is available in Table S2.

4 | DISCUSSION

4.1 | Increases in aridity lead to dramatic changes in the assembly of soil microbial communities

Our findings support the hypothesis that increases in aridity lead to significant changes in the relative abundance of modules of tightly co-occurring fungal and bacterial phylotypes. In particular, our results indicate that certain microbial modules will be susceptible to increases in aridity, particularly in the transition between semiarid and arid areas (where Mesic Module #1 shifted to Xeric Module #2). Previous studies have shown that increases in aridity negatively affect microbial diversity and abundance (Maestre et al., 2015). Here, we provide solid

evidence that increases in aridity, just as those predicted under climate change, can promote marked changes in the assembly of complex microbial networks at the regional scale, leading to substantial turnover of entire microbial communities. These changes may result in local extinctions in terrestrial ecosystems. Moreover, we were able to identify particular taxa of fungi and bacteria at the OTU level (phylotype level) that are strongly negatively (losers) or positively (winners) related to increases in aridity in eastern Australia. These results provide a regional list of particular microbial phylotypes that could be highly vulnerable to predicted increases in aridity in this century. These results have implications for our understanding of processes related to land degradation and desertification, such as overgrazing and land clearance, which are likely to become more pronounced as we move to a drier and more unpredictable climate.

An important result from our study was that increases in aridity shifted the network of associations from a dominance by fungal phylotypes (in terms of OTU relative abundance and number of phylotypes) associated with bacteria (Mesic Module #1) to bacterial phylotypes co-occurring with fungi (Xeric Module #2). In support of these results, our SEM showed that the fungal:bacterial ratio declined with increasing aridity. Soil bacteria and fungi include mutualistic, neutral, pathogenic, and parasitic relationships, and their complex associations are linked to essential ecosystem processes such as litter decomposition (Kobayashi & Crouch, 2009). Changes in the relative contribution of phylotypes of bacteria and fungi to the network of microbial associations might then alter soil functioning in terrestrial ecosystems. Bacteria and fungi are known to be involved in different processes that are fundamental for sustaining a functional ecosystem (van der Heijden, Bardgett, & van Straalen, 2008). For example, bacterial-dominated microbial communities often lead to fast cycling of nutrient (e.g., nitrification) and to open nutrient cycling (i.e., lower capacity to retain nutrients in the system; van der Heijden et al., 2008). Moreover, slow-growing organisms such as soil fungi have been reported to promote the resistance of nutrient cycling to climate change compared with fast-growing organisms such as bacteria (van der Heijden et al., 2008). Thus, by promoting changes in the contribution of bacteria over fungi phylotypes to the network of associations, increases in aridity might indirectly impact the provision and resistance of essential ecosystem functions and services such as litter decomposition and nutrient cycling (Kobayashi & Crouch, 2009).

4.2 | Direct and indirect effects of aridity on the relative abundance of microbial modules

We found that aridity regulated the relative abundance of main microbial modules both directly, that is, via reductions in water availability, and indirectly via changes in soil type, soil properties such as soil P and pH, and total plant cover, which are known to be impacted by aridity (Delgado-Baquerizo et al., 2013; Maestre et al., 2015). Part of these effects might be associated with the fact that soils in Australian drylands are old, acidic, and nutrient-depleted, compared with other drylands (Eldridge, Maestre, Koen, & Delgado-Baquerizo, 2018). For example, increases in soil pH associated with increasing aridity may

explain the observed changes in the assembly of these networks. Soil pH has been widely reported to be an important driver of microbial communities in terrestrial ecosystems. However, this is not always the case for drylands where pH is typically high, and microbial communities are less sensitive to changes in pH (Maestre et al., 2015; Neilson et al., 2017). Similarly, increases in soil P with aridity may play a major role in driving the soil microbial networks studied, as Australian environments are known to be strongly P-limited, with reported consequences for the biodiversity and functioning of biotic communities (Lambers et al., 2013). Reductions in plant cover associated with increases in aridity might also alter the complete microbial network of associations via reductions in resource inputs (e.g., litter and rhizodeposition) and exacerbating specific harsh environmental conditions (e.g., amount of radiation). Our findings indicate that soil variables such as pH and total P—linked to changes in soil type with increases in aridity—and plant cover, which are important predictors of microbial community composition and diversity (Maestre et al., 2015; Tedersoo et al., 2014), are also key drivers of the complex network of bacterial and fungal phylotypes associations in soils. Some of these findings have strong implications for forecasting climate change impacts on microbial networks. For example, trees had indirect negative and positive effects, respectively, on Mesic Module #1 and Xeric Module #2 via soil pH and soil P. Interestingly, plant cover and richness had multiple direct effects on the relative abundance of Mesic Module #1 and Xeric Module #2. These results highlight the importance of microsite differentiation in controlling the assembly of complex microbial networks via changes in local soil properties. Moreover, this result further suggests that changes in vegetation functional composition in response to increasing aridity will have indirect consequences for the relative abundance of key microbial modules in terrestrial environments. For example, increases in aridity are linked to reduced cover of trees (Table S3). Further, the cover of trees was positively or negatively linked to the relative abundance of Mesic Module #1 and Xeric Module #2, respectively (Table S3). Thus, changes in the relative abundance of this within-plot vegetation type could impact the assembly of microbial networks in terrestrial ecosystems, with potential collateral effects for ecosystem functioning. These results are in accordance with a recent study evaluating changes in microbial diversity along a regional aridity gradient in Chile (Neilson et al., 2017).

Our SEM model supports the hypothesis that increasing aridity will lead to the turnover of entire microbial communities in terrestrial ecosystems by shifting the relative abundance of well-defined microbial modules (from Mesic Module #1 to Xeric Module #2). Given the observed links between network structure and ecosystem functioning, we expect these shifts to have strong implications for ecosystem functioning under a changing climate. For example, we found that the relative abundance of Mesic Module #1 was positively related to variables such as the activity of phosphatase and the amount of available soil C and inorganic N and ANPP, which are all linked to ecosystem functions and services such as nutrient cycling, organic matter decomposition and mineralization, and food production (Table S1). Thus, our results propose the idea that changes in the complex network of

microbial associations derived from increased aridity might negatively impact ecosystem processes linked to the provision of key ecosystem services. Moreover, these findings further support the results of a previous metagenomics study reporting large differences in potential soil functioning between arid and humid environments (Fierer et al., 2012). Future endeavors exploring modules of microbial communities co-occurring in terrestrial ecosystems should further evaluate the functional attributes of microbial modules so that we can gain further functional insights on the role of microbial networks in regulating ecosystem functioning.

4.3 | Winners and losers microbial taxa in response to increasing aridity

We identified microbial taxa that are potentially vulnerable (losers) or might benefit (winners) from predicted increases in aridity throughout this century (Huang et al., 2016; Neilson et al., 2017). Microbial losers are expected to be phylotypes unable to tolerate the increasingly harsh conditions associated with aridity, including water scarcity or extreme radiation derived from reductions in plant coverage. Here, we found that increases in aridity may reduce the relative abundance of some microbial phylotypes within Mesic Module #1, which are linked to the performance of plants via symbiosis such as *Burkholderia tuberum* (capable of symbiotic nitrogen fixation with some legumes; Esqueda et al., 2012) and *Oidiodendron* sp. (ericoid mycorrhiza; Smith & Read, 2008). In addition, we found that important taxa such as *Helotiales* sp. (saprobies) and *Sphingomonas wittichii* (involved in toxin degradation) might be negatively influenced by increases in aridity, with consequences for overall ecosystem functioning. Interestingly, the parasitic nematode *Pochonia bulbillosa* was also found to decline with increases in aridity, suggesting that, as found with soil animals and vascular plants (Vicente-Serrano et al., 2012), associated microbial phylotypes will also be negatively impacted by increases in aridity.

We also found multiple phylotypes whose relative abundance increased with aridity. Winners, that is, phylotypes which can potentially benefit from increases in aridity along this century, are expected to be thermophilic and highly resistant to desiccation and radiation. Interestingly, taxa from Xeric Module #2 included a wide variety of taxa typical from desert ecosystems, which are noted radiation and desiccation tolerant desert bacteria including phylotypes from the genus *Rubrobacter*, *Geodermatophilus*, and *Streptomyces* or from the class *Thermomicrobia* (Mohammadipanah & Wink, 2016). All these taxa were strongly positively correlated with aridity. We also found fungal phylotypes typical from drylands, such as *Tulostoma melanocyclum*, *Preussia minima*, and *Geastrum pectinatum*, to be strongly positively related to aridity (Esqueda et al., 2004). We also found that increasing aridity had a strong positive correlation with the relative abundance of multiple fungal pathogens of plants, including *Alternaria triticumaculans*, *Pleosporales* sp., *Pleosporaceae* sp., *Fusarium tricinctum*, and *Phoma macrostoma*. We also found that the relative abundance of *Mortierella wolfii*, a well-known pathogen of humans and other animals that can cause bovine abortion and pneumonia (Davies & Wobeser, 2010), increased with aridity. Other fungal taxa such as *Capronia*

peltigerae—a parasite of living lichens—also increased in the most arid places, where biocrust-forming lichens are often abundant (Liu et al., 2017). Building on from previous efforts aiming to identify the role of aridity in regulating microbial communities in drylands (Maestre et al., 2015; Neilson et al., 2017), our study improves our understanding and provides evidence for potential winner and loser taxa in response to increases in aridity in Australia.

5 | CONCLUSIONS

All things considered, our findings present strong evidence that increases in aridity will lead to critical shifts in the assembly of complex microbial networks of fungi and bacteria, potentially leading to massive phylotype exchange and local extinctions in terrestrial ecosystems, as demonstrated by the reductions of up to 97% in the relative abundance of microbial taxa within Mesic Module #1. Our results thus fill major gaps in our understanding of how complex networks of microbial associations respond to increases in aridity, which will promote land degradation in drylands worldwide, and provide solid evidence of the vulnerability of microbial networks to climate change. Considering the primacy of microbial communities in ecosystem functioning, the reported changes in the assembly of microbial co-occurrence networks are likely to have far-reaching consequences for the provision of important ecosystem functions and services like litter breakdown, nutrient cycling, and plant productivity and, hence, need to be considered when assessing the consequences of climate change and associated land degradation on the functioning of terrestrial ecosystems.

ACKNOWLEDGMENTS

This research is supported by the Australian Research Council projects DP190103714 and DP170104634. We thank Melissa S. Martin for revising the English of this manuscript. D.B.S. acknowledges the support of a Marsden Fast-Start Grant and a Rutherford Discovery Fellowship, both administered by the Royal Society of New Zealand. M.D.-B. acknowledges support from the Marie Skłodowska-Curie Actions of the Horizon 2020 Framework Programme H2020-MSCA-IF-2016 under REA Grant 702057. D.J.E. was supported by the Hermon Slade Foundation. F.T.M. acknowledges support from the European Research Council (BIODESERT project, ERC Grant 647038), the Spanish Ministerio de Economía y Competitividad (BIOMOD project, ref. CGL2013-44661-R), and from a Humboldt Research Award from the Alexander von Humboldt Foundation.

AUTHOR CONTRIBUTIONS

M.D.-B. designed this study in consultation with D.B.S. Field data were collected by M.D.-B. and D.J.E. Soil analyses were conducted by F.T.M. Sequencing data were provided by B.K.S. Bioinformatic analyses were done by T.C.J. Network analyses were done by D.B.S., G.D., and J.W. in consultation with J. R. P. The manuscript was written by M. D.-B., edited by D. J. E., B. K. S., D. B. S., and F. T. M., and all authors contributed substantially to the revisions.

DATA ACCESSIBILITY

The primary data have been deposited in figshare: <https://figshare.com/s/5c12e197707e753dbfaa> (DOI: 10.6084/m9.figshare.7571399). The raw sequence data have been deposited in figshare: <https://figshare.com/s/55813554972fd4a51195> (DOI: 10.6084/m9.figshare.7092950).

ORCID

Manuel Delgado-Baquerizo  <https://orcid.org/0000-0002-6499-576X>

David J. Eldridge  <https://orcid.org/0000-0002-2191-486X>

Daniel B. Stouffer  <https://orcid.org/0000-0001-9436-9674>

Fernando T. Maestre  <https://orcid.org/0000-0002-7434-4856>

Juntao Wang  <https://orcid.org/0000-0002-1822-2176>

Jeff R. Powell  <https://orcid.org/0000-0003-1091-2452>

Brajesh K. Singh  <https://orcid.org/0000-0003-4413-4185>

REFERENCES

- Barberán, A., Bates, S. T., Casamayor, E. O., & Fierer, N. (2012). Using network analysis to explore co-occurrence patterns in soil microbial communities. *ISME Journal*, 6, 343–351.
- Bell, C. W., Fricks, B. E., Rocca, J. D., Steinweg, J. M., McMahon, S. K., & Wallenstein, M. D. (2013). High-throughput fluorometric measurement of potential soil extracellular enzyme activities. *Journal of Visualized Experiments*, 81, e50961.
- Caporaso, J. G., Kuczynski, J., Stombaugh, J., Bittinger, K., Bushman, F. D., Costello, E. K., ... Knight, R. (2010). QIIME allows analysis of high-throughput community sequencing data. *Nature Methods*, 7, 335–336.
- Davies, J. L., & Wobeser, G. A. (2010). Systemic infection with *Mortierella wolffii* following abortion in a cow. *Canadian Veterinary Journal*, 51, 1391–1393.
- Delgado-Baquerizo, M., Maestre, F. T., Gallardo, A., Bowker, M. A., Wallenstein, M. D., Quero, J. L., ... Zaady, E. (2013). Decoupling of soil nutrient cycles as a function of aridity in global drylands. *Nature*, 502, 672–676.
- Delgado-Baquerizo, M., Eldridge, D. J., Ochoa, V., Gozalo, B., Singh, B. K., & Maestre, F. T. (2017). Soil microbial communities drive the resistance of ecosystem multifunctionality to global change in drylands across the globe. *Ecology Letters*, 20, 1295–1305.
- Delgado-Baquerizo, M., Maestre, F. T., Reich, P. B., Trivedi, P., Osanai, Y., Liu, Y., ... Singh, B. K. (2016). Carbon content and climate variability drive global soil bacterial diversity patterns. *Ecological Monographs*, 3, 373–390.
- Delgado-Baquerizo, M., Oliverio, A. M., Brewer, T. E., Benavent-González, A., Eldridge, D. J., Bardgett, R. D., ... Fierer, N. (2018). A global atlas of the dominant bacteria found in soil. *Science*, 359(6373), 320–325.
- DeSantis, T. Z., Hugenholtz, P., Larsen, N., Rojas, M., Brodie, E. L., Keller, K., ... Andersen, G. L. (2006). Greengenes, a chimera-checked 16S rRNA gene database and workbench compatible with ARB. *Applied and Environmental Microbiology*, 72, 5069–5072.
- Edgar, R. C. (2010). Search and clustering orders of magnitude faster than BLAST. *Bioinformatics*, 26, 2460.
- Eldridge, D. J., Delgado-Baquerizo, M., Travers, S. K., Val, J., & Oliver, I. (2018). Livestock grazing and forest structure regulate the assembly of ecological clusters within plant networks in eastern Australia. *Journal of Vegetation Science*, 29, 788–797.
- Eldridge, D. J., Maestre, F. T., Koen, B., & Delgado-Baquerizo, M. (2018). Australian dryland soils are acidic and nutrient-depleted, and have unique microbial communities compared with other drylands. *Journal of Biogeography*, 45, 2803–2814.
- Fierer, N., Leff, J. W., Adams, B. J., Nielsen, U. N., Bates, S. T., Lauber, C. L., ... Caporaso, J. G. (2012). Cross-biome metagenomic analyses of soil microbial communities and their functional attributes. *Proceedings of the National Academy of Sciences of the United States of America*, 109, 21390–21395.
- Friedman, J., & Alm, E. J. (2017). Inferring correlation networks from genomic survey data. *PLOS Computational Biology*, 8, e1002687.
- Grace, J. B. (2006). *Structural equation modeling natural systems*. Cambridge, UK: Cambridge University Press.
- Huang, J., Yu, H., Guan, X., Wang, G., & Guo, R. (2016). Accelerated dryland expansion under climate change. *Nature Climate Change*, 6, 166–171.
- Liu, Y.-R., Delgado-Baquerizo, M., Trivedi, P., He, Y.-Z., Wang, J.-T., & Singh, B.-K. (2017). Identity of biocrust species and microbial communities drive the response of soil multifunctionality to simulated global change. *Soil Biology and Biochemistry*, 107, 208–217.
- Maestre, F. T., Delgado-Baquerizo, M., Jeffries, T. C., Eldridge, D. J., Ochoa, V., Gozalo, B., ... Singh, B. K. (2015). Increasing aridity reduces soil microbial diversity and abundance in global drylands. *Proceedings of the National Academy of Sciences of the United States of America*, 112, 15684–15689.
- Mohammadipanah, F., & Wink, J. (2016). Actinobacteria from arid and desert habitats: Diversity and biological activity. *Frontiers in Microbiology*, 6, 1541.
- Neilson, J. W., Califf, K., Cardona, C., Copeland, A., van Treuren, W., Josephson, K. L., ... Maier, R. M. (2017). Significant impacts of increasing aridity on the arid soil microbiome. *mSystems*, 30, e00195–e00216.
- Newman, M. E. J., & Girvan, M. (2004). Finding and evaluating community structure in networks. *Physical Review*, 69, 26113.
- Shi, S., Nuccio, E. E., Shi, Z. J., He, Z., Zhou, J., & Firestone, M. K. (2016). The interconnected rhizosphere: High network complexity dominates rhizosphere assemblages. *Ecology Letters*, 6, 926–936.
- Smith, S. E., Read, D. J. (2008). *Mycorrhizal symbiosis*, Third Edition. Academic Press.
- Stouffer, D. B., & Bascompte, J. (2011). Compartmentalization increases food-web persistence. *Proceedings of the National Academy of Sciences of the United States of America*, 108, 3648–3652.
- Tedersoo, L., Bahram, M., Põlme, S., Kõljalg, U., Yorou, N. S., Wijesundera, R., ... Abarenkov, K. (2014). Fungal biogeography global diversity and geography of soil fungi. *Science*, 28, 346.
- van der Heijden, M. G., Bardgett, R. D., & van Straalen, N. M. (2008). The unseen majority, soil microbes as drivers of plant diversity and productivity in terrestrial ecosystems. *Ecology Letters*, 11, 296–310.
- van Dongen, S.M. (2000). Graph clustering by flow simulation. Ph.D. thesis, University of Utrecht.
- Vincent, P., Larochelle, H., Bengio, Y., Manzagol, P.-A. Extracting and composing robust features with denoising autoencoders (2008). In Proceedings of the 25th International Conference on Machine learning. ACM, pp. 1096–1103 Retrieved from <http://dl.acm.org/citation.cfm?id=1390294>.
- Vicente-Serrano, S. M., Gouveia, C., Camarero, J. J., Beguería, S., Trigo, R., López-Moreno, J. I., ... Sanchez-Lorenzo, A. (2012). Response of vegetation to drought time-scales across global land biomes. *Proceedings of the National Academy of Sciences of the United States of America*, 110, 52–57.

SUPPORTING INFORMATION

Additional supporting information may be found online in the Supporting Information section at the end of this article.

How to cite this article: Delgado-Baquerizo M, Doulcier G, Eldridge DJ, et al. Increases in aridity lead to drastic shifts in the assembly of dryland complex microbial networks. *Land Degrad Dev*. 2020;31:346–355. <https://doi.org/10.1002/ldr.3453>